Mohammedi Mohammed Nourelislam[1], Benfrid Abdelmoutalib[1], Benatta Mohamed Atef[1], Bachir Bouiadjra Mohamed[1,2],Krour Baghdad[1]*

[1]Laboratory of Advanced Structures and Materials in Civil Engineering and Public Works, Sidi Bel Abbes, Algeria, [2]Thematic Agency for Research in Science and Technology (ATRST), 16000 Algiers, Algeria

Scientific paper
ISSN 0351-9465, E-ISSN 2466-2585
https://doi.org/10.62638/ZasMat1851

Zastita Materijala 67 ()
(2026)

Effective mechanical properties of eco-concretes reinforced with bio-sourced calcium carbonate nanoparticles: Free vibration analysis of simply supported slabs

ABSTRACT

Bio-sourced calcium carbonate-rich wastes, such as eggshells, fish bones, animal bones, and snail shells, represent promising raw materials for producing calcium carbonate nanoparticles after suitable processing, such as grinding, calcination, or chemical precipitation. In this study, the effective mechanical properties and free vibration response of simply supported eco-concrete slabs reinforced with bio-sourced calcium carbonate nanoparticles are investigated.

The effective elastic properties of the concrete composite are evaluated using the Hashin–Shtrikman homogenization model for a two-phase isotropic system composed of concrete as the matrix and nano-$CaCO_3$ particles as the reinforcement. Reinforcement volume fractions of 10% and 20% are considered. The free vibration behavior of the reinforced slabs is then analyzed using First-Order Shear Deformation Theory (FSDT) and Higher-Order Shear Deformation Theory (HSDT). The governing equations are derived using the principle of virtual work, and Navier's analytical solution is adopted to satisfy the simply supported boundary conditions.

The obtained results show that the addition of nano-$CaCO_3$ improves the effective stiffness of concrete. The Young's modulus increases from 20 GPa for ordinary concrete to 22.81 GPa and 25.88 GPa for 10% and 20% nano-$CaCO_3$ reinforcement, respectively. The fundamental dimensionless frequency of the square slab increases from 0.0921 for ordinary concrete to 0.1277 and 0.1287 for 10% and 20% nano-$CaCO_3$, respectively. These results indicate that 10% nano-$CaCO_3$ provides a significant improvement in stiffness and vibration performance, while the additional gain beyond this fraction remains limited. The HSDT formulation shows better agreement with reference results than FSDT and is therefore adopted for the parametric analysis.

Keywords: *Eco-concrete; bio-sourced calcium carbonate; nano-$CaCO_3$; Hashin–Shtrikman model; simply supported slab; free vibration; HSDT.*

1. INTRODUCTION

Nanoparticle- based technologies have attracted increasing attention in civil engineering materials because of their ability to improve the effective mechanical performance of cementitious composites. Concrete, as one of the most widely used construction materials, can benefit from the incorporation of nano-sized particles through improvements in stiffness, durability, and structural performance. In this context, several analytical and numerical studies have investigated the behavior of nanoparticle-reinforced concrete using homo genization approaches.

Harrat et al. [1] studied the static behavior of concrete beams reinforced with nano-SiO_2 and resting on an elastic foundation. Their work showed that the incorporation of nano-silica can improve the stiffness of concrete beams and reduce deflection. Chatbi et al. [2] analyzed the bending response of nano-SiO_2 -reinforced concrete slabs and highlighted the influence of reinforcement distribution and foundation parameters on the structural response. Benfrid et al. [3] investigated eco-concrete panels reinforced with glass powder and evaluated their thermo-mechanical performance, showing the potential of waste-derived particles for sustainable construction. Elhennani et al. [4] examined the buckling and free vibration behavior of concrete beams reinforced with different mineral nanoparticles and resting on multi-parameter elastic foundations. Kecir et al. [5]

*Corresponding author: Benfrid Abdelmoutalib
E-mail: benfridabdelmoutalib2050@gmail.com
Paper received: 22.04.2026.
Paper accepted: 05.05.2026.

studied concrete slabs reinforced with nano-sized iron oxide particles and demonstrated that $Fe_2\ O_3$ nanoparticles can improve the effective stiffness and bending resistance of the concrete system.

In parallel with nanotechnology development, the use of bio-sourced and waste-derived materials in concrete has become an important research direction for sustainable construction. Jaramillo et al. [6] presented a bibliometric review on biomaterials used in concrete and showed the growing scientific interest in bio-based materials for engineering applications. Schmidt et al. [7] investigated self-compacting and high-performance concretes incorporating rice husk ash, cassava starch, lignosulfonate, and sisal fibers, and reported improvements in durability. Kawaai et al. [8] studied bio-based additives such as alginate and Bacillus subtilis for crack repair mortars and showed their ability to reduce capillary absorption and improve crack-sealing performance. Fatahillah and Sumarno [9] examined the combined use of fly ash and chicken eggshell powder as cement substitutes and reported improvements in compressive strength at suitable replacement levels.

Several experimental studies have also confirmed the mechanical benefits of calcium-rich bio-sourced materials in cementitious composites. Zaid et al. [10] showed that eggshell powder combined with nano-silica can enhance the strength of ultra-high-performance fiber-reinforced concrete, especially at 5% and 10% contents, while higher contents may reduce performance. Shcherban' et al. [11] investigated eco-friendly concrete modified with eggshell powder and identified 10% as an efficient dosage for reducing deformation under compression and tension. Bhat et al. [12] demonstrated that crushed animal bones can be used as partial replacement of coarse aggregates in lightweight concrete, reaching compressive strengths of about 20 MPa. Claudius et al. [13] studied pulverized animal bones and animal bone ash and showed that these materials can improve the mechanical properties of normal-strength concrete. Damayanti et al. [14] investigated fishbone fiber and rice husk ash additives and confirmed that these materials can maintain acceptable mechanical performance in concrete. Arain et al. [15] showed that fish scales can be used as sustainable reinforcement in cement concrete and can improve concrete properties at suitable contents. Sulaiman et al. [16] studied fish scale powder as a sustainable blending material and highlighted its environmental benefits. Higashino et al. [17] developed porous concrete mixed with hydroxyapatite produced from fish bones and showed that calcium-rich fish-bone-derived materials can enhance concrete performance. Yanaka et al. [18] investigated fishery waste in porous concrete and showed its potential for carbon-neutral and sustainable construction applications.

Among calcium-rich bio-sourced wastes, eggshells, fish bones, animal bones, and shells are especially relevant because they contain large amounts of calcium carbonate. However, calcium carbonate nanoparticles are not directly present in these raw wastes. These materials should instead be considered as calcium-carbonate-rich bio-sources from which nano-$CaCO_3$ particles can be produced after suitable processing methods, such as cleaning, drying, grinding, calcination, ball milling, or chemical precipitation. In the present study, waste eggshells are considered as the representative bio-sourced calcium carbonate material because they are mainly composed of calcium carbonate and have been widely investigated as a sustainable resource for cementitious applications. Lecompte et al. [33] studied animal-bone-derived calcium phosphate particles and demonstrated the potential of animal waste for producing functional mineral particles. Tiwari et al. [34] reviewed methods for converting biomass waste into value-added nanomaterials, showing that bio-waste can be transformed into useful engineering materials. Hussin et al. [35] reviewed high-performance bio-based materials and highlighted the importance of waste valorization in sustainable material development.

In addition to mechanical performance, the dynamic behavior of concrete structures is a key issue in structural engineering. Slabs, plates, beams, foundations, and shell elements are frequently subjected to dynamic actions caused by wind, traffic, machinery, seismic activity, and environmental vibrations. Therefore, understanding their free vibration response is essential for safe and reliable structural design. Ding et al. [19] developed a mathematical formulation for bending, vibration, and stability analysis of laminated rectangular plates with transversely isotropic layers. Alfano and Pagnotta [20] proposed a modal vibration testing approach to determine the elastic constants of isotropic materials from natural frequencies of rectangular plates. Turan [21] investigated the natural frequencies of porous orthotropic laminated doubly curved shallow shells using higher-order shear deformation theory. Turan et al. [22] extended this approach to analyze free vibration and buckling of porous orthotropic shallow shells under non-uniform compression. Turan [23] studied multi-layered porous plates with trigonometric porosity distribution and demonstrated the influence of porosity distribution on natural frequencies. Bahadır and Turan [24]

analyzed laminated cylindrical panels with non-uniform porosity and showed the importance of porosity configuration in vibration response. Turan [25] investigated porous cylindrical panels resting on elastic foundations and highlighted the effect of foundation stiffness on vibration behavior. Turan [26] studied porous orthotropic two-layered plates and confirmed the relevance of shear deformation theory in predicting natural frequencies.

Several studies have also focused on structural dynamics, seismic effects, elastic foundations, and beam vibration. Doicheva and Mladenov [27] investigated dynamic characteristics of building structures and emphasized the importance of vibration parameters in structural assessment. Rizov et al. [28] analyzed a pedestrian bridge with respect to Eurocode comfort requirements and showed the importance of vibration control in serviceability design. Işık [29] studied the strengthening of reinforced concrete structural elements using fiber-based polymers and showed that such reinforcement can improve seismic resistance. Ike [30] applied the Ritz variational method to study free harmonic vibration of beams on two-parameter elastic foundations. Ike [31] used the Stodola–Vianello iteration method to solve lateral-torsional buckling problems of thin-walled beams. Ike [32] also applied the Stodola–Vianello method to Euler–Bernoulli beams resting on Winkler foundations, demonstrating its applicability to transverse vibration problems.

The Hashin–Shtrikman homogenization model is particularly suitable for estimating the effective elastic properties of isotropic two-phase composites because it provides rigorous upper and lower bounds for the bulk and shear moduli. Hashin and Shtrikman [36] established a variational approach for predicting the elastic behavior of multiphase materials, which remains a fundamental reference in homogenization theory. Shi et al. [37] proposed an interphase model for the effective elastic properties of concrete composites and showed the importance of the interfacial zone in homogenization. Dong et al. [38] used asymptotic homogenization to evaluate effective thermal-elastic properties of concrete considering its three-dimensional mesostructure. Wall [39] compared homogenization approaches, Hashin–Shtrikman bounds, and Halpin–Tsai equations, showing the relevance of bounds-based models. Kurukuri [40] studied homogenization of damaged concrete mesostructures using representative volume elements and confirmed the usefulness of homogenization methods for concrete materials.

Recent works have combined homogenization methods with refined structural theories to evaluate the mechanical, thermal, and dynamic behavior of cementitious and composite materials. Benfrid and Murawski [41] investigated eco-concrete beams reinforced with waste pottery and showed that waste-based reinforcement can modify thermo-mechanical behavior. Lee and Cohen [42] studied the influence of cement paste–aggregate interfaces on concrete strength and durability, highlighting the importance of transition zones. Luciano and Willis [43] combined Hashin–Shtrikman-based finite element analysis with random composite modeling to study elastic behavior. Aouissi et al. [44] compared biphasic and triphasic models for predicting concrete elastic modulus and showed the influence of modeling assumptions. Shi et al. [45] further emphasized the role of micromechanical modeling and interphase effects in concrete composites. Avhad and Sayyad [46] developed a higher-order beam theory for sandwich beams, contributing to refined structural modeling. Benfrid et al. [47] studied glass nanoparticles in concrete and showed their effect on elastic modulus. Ekpraseert et al. [48] investigated $CaCO_3$ precipitated by bacteria and its mechanical and biocement applications, providing useful data for calcium carbonate-based materials. Ghugal and Sayyad [49] studied free vibration of thick isotropic plates using trigonometric shear deformation theory, providing reference results for validation. Sayyad et al. [50] analyzed bending and free vibration of isotropic plates using refined plate theory, which is relevant for plate vibration formulations.

Other studies have addressed waste recycling, pozzolanic additives, sustainable cementitious composites, and innovative concrete formulations. Kaewsit et al. [51] studied lightweight expanded clay aggregates produced from industrial waste and showed their potential for sustainable construction. Zhang et al. [52] developed a piezoelectric stick-slip actuator, contributing to advanced material and mechanical system design. Chareerat et al. [53] investigated porous concrete-based hydroponic systems and showed the influence of aggregate size and void ratio. Dechboon et al. [54] studied the reuse of kaolin waste and longan wood ash in ceramic glazes, highlighting broader waste valorization strategies. Bello et al. [55] analyzed biomass and plastic waste blends for bio-oil production, contributing to circular economy approaches.

Al-Ani et al. [56] investigated the static and dynamic behavior of bridge decks reinforced with nanoparticles and showed that nano-reinforcement can improve dynamic performance. Benfrid et al. [57] studied waste-derived glass nanopowders in structural wall concrete and reported improvements

in thermal efficiency and mechanical properties. Harrat et al. [58] analyzed nano-Fe_2O_3-reinforced concrete slabs exposed to temperature fields and resting on a viscoelastic foundation, showing that nanoparticles and foundation parameters strongly influence slab behavior. Lakhder et al. [59] studied nanocomposite plates reinforced with tungsten nanoparticles and showed the effect of nano-reinforcement on bending behavior. Chatbi et al. [60] investigated concrete beams reinforced with nano-clay platelets and demonstrated improved bending performance on elastic foundations.

Several complementary studies have investigated advanced materials, sustainable concrete formulations, structural dynamics, soil–structure interaction, waste valorization, and reinforced structural elements. Ahmed et al. [61] used first-principles calculations to study hydride perovskites and provided insight into their electronic and elastic properties. Bouchehit et al. [62] analyzed cylindrical and rectangular oil tanks under soil–structure–fluid interaction and showed the influence of wall thickness and support conditions on seismic behavior. Ahmed et al. [63] studied concrete beams incorporating granite waste and reported improved flexural performance. Yerkrou et al. [64] proposed a programming model for mechanical and thermal buckling of eco-concrete panels incorporating glass and red-brick wastes. Abdelmoutalib et al. [65] investigated thermal instability of polymer panels reinforced with glass particulates. Benfrid [66] proposed a biphasic homogenization approach for predicting thermal and mechanical properties of eco-concretes. Belmahi et al. [67] studied the influence of acidic and alkaline environments on cement mortar properties. Benfrid [68] investigated concrete expanded with aluminum nano-inclusions and evaluated its elastomechanical properties. Khetir et al. [69] studied lightweight concrete beams reinforced with bio-sourced nanocomposites and showed improved mechanical performance. Chatbi et al. [70] analyzed nano-clay platelet effects on concrete beam bending response. Harrat et al. [71] modeled dynamic response of clay nanoparticle-modified concrete beams on two-parameter elastic foundations. Zahafi et al. [72] proposed a lumped-parameter model for vertical vibrations of circular foundations on nonhomogeneous soil. Bencharif et al. [73] implemented soil–structure interaction techniques using frequency-dependent impedance functions. Chatbi et al. [74] studied silica nanoparticle-reinforced concrete slabs on elastic and viscoelastic foundations. Chatbi et al. [75] investigated free vibration of carbon-nanotube-reinforced composite beams on elastic foundations. Bencharif et al. [76] developed a hybrid BEM–TLM–PML method for impedance functions of strip footings. Tebbouche et al. [77] characterized the El Kherba landslide after the Mila earthquake using field observations and ambient noise analysis.

Further studies have addressed sustainable construction, homogenization, and structural mechanics. Benfrid [78] compared homogenization models for environmental concretes. Sid Ahmed et al. [79] studied thermally treated plastic-pozzolanic mortars and their mechanical properties. Sid Ahmed et al. [80] developed eco-friendly composite mortars for circular economy and sustainable construction. Turan and Benfrid [81] investigated free vibration of porous orthotropic beams. Benfrid [82] studied free vibration of raft foundations reinforced with short steel fibers. Benfrid and Turan [83] investigated heat transfer in eco-friendly concrete panels with recycled cardboard. Mladenov and Doicheva [84] examined simply supported beams and their illustrative structural behavior. Mladenov and Doicheva [85] analyzed flexural-torsional buckling of off-center supported beams. Doicheva [86] proposed an exact solution for beams on off-center spring supports. Doicheva [87] analyzed the critical and post-critical response of T-shaped frames. Mladenov and Doicheva [88] investigated water towers with conical tanks under critical and post-critical behavior. Mladenov and Doicheva [89] studied bending-torsional buckling of beams on elastic rotational springs. Doicheva and Mladenov [90] analyzed dynamic characteristics in building structures. Doicheva [91–95] investigated shear force behavior in reinforced concrete beam-column joints under different loading configurations and crack development. The study reported in [96] proposed an approach for plaster beam bending using nano-short-bio-fibers. Benfrid et al. [97] studied thermal insulation using bio-based concrete made from apricot kernels. Benfrid et al. [98] investigated wheat straw nanofibers for improving thermal efficiency of bio-concrete. Additional studies by Benfrid and co-workers [99,100] focused on sustainable nano-reinforced concrete panels and homogenization-based prediction of effective properties of bio-sourced concrete composites.

Despite the large number of studies on bio-sourced materials, nano-reinforced concrete, homogenization models, and structural vibration, limited attention has been given to the analytical prediction of the effective mechanical properties of eco-concrete reinforced with bio-sourced nano-$CaCO_3$ particles and to the influence of these effective properties on the free vibration response of simply supported concrete slabs. Most available studies focus either on experimental strength and durability of bio-based concrete or on conventional nano-additives such as nano-silica, nano-clay, nano-Fe_2O_3, glass nanopowder, and carbon

nanotubes. Therefore, a clear research gap remains in linking bio-sourced nano-$CaCO_3$ reinforcement, effective mechanical property prediction, and free vibration analysis of simply supported slabs within a unified analytical framework.

The present study aims to investigate the effective mechanical properties and free vibration behavior of simply supported eco-concrete slabs reinforced with bio-sourced calcium carbonate nanoparticles. The concrete is modeled as a two-phase isotropic composite composed of ordinary concrete as the matrix and nano-$CaCO_3$ particles as the reinforcing phase. The effective Young's modulus, shear modulus, bulk modulus, Poisson's ratio, and density are evaluated using the Hashin–Shtrikman homogenization model. Reinforcement volume fractions of 10% and 20% are considered. The obtained effective properties are then introduced into the free vibration formulation of simply supported concrete slabs.

The vibration problem is formulated using First-Order Shear Deformation Theory (FSDT) and Higher-Order Shear Deformation Theory (HSDT). The governing equations are derived using the principle of virtual work, and Navier's analytical solution is adopted to satisfy the simply supported boundary conditions. The accuracy of the formulation is verified through comparison with reference results from the literature. The novelty of this study lies in combining the Hashin–Shtrikman homogenization model with refined plate theories to evaluate the influence of bio-sourced nano-$CaCO_3$ particles on both the effective mechanical properties and the free vibration response of simply supported eco-concrete slabs. This work provides an analytical framework linking sustainable nano-reinforcement, effective stiffness improvement, and vibration performance of eco-concrete structural elements.

2. HOMOGENIZATION AND FREE VIBRATION FORMULATION OF SIMPLY SUPPORTED ECO-CONCRETE SLABS

The present section presents the analytical formulation used to evaluate the effective mechanical properties and the free vibration response of simply supported eco-concrete slabs reinforced with bio-sourced nano-$CaCO_3$ particles. The procedure is based on two complementary steps. First, the effective elastic properties of the reinforced concrete are estimated using the Hashin–Shtrikman homogenization model. Second, these effective properties are introduced into the governing equations of the simply supported slab in order to determine its natural frequencies using shear deformation plate theories.The following assumptions are adopted in the homogenization procedure.

2.1. Effective properties using the Hashin–Shtrikman model

The Hashin–Shtrikman model [36] is widely used for estimating the effective elastic properties of isotropic heterogeneous materials. This model provides rigorous upper and lower bounds for the effective bulk and shear moduli of multiphase composites. Compared with the Voigt and Reuss models, which are based on uniform strain and uniform stress assumptions, respectively, the Hashin–Shtrikman bounds provide a more realistic estimation for heterogeneous materials such as concrete.

The applicability of the Hashin–Shtrikman model to concrete and cementitious composites has been reported in several studies. Benfrid et al. [41] used this model to homogenize concrete reinforced with glass nanoparticles. Zhang et al. [42] applied a homogenization approach to investigate the interfacial transition zone and durability of concrete. Luciano and Willis [43] combined Hashin–Shtrikman-based estimates with finite element analysis to study non-local interactions in composite materials. Aouissi et al. [44] compared biphasic and triphasic models for predicting the elastic modulus of concrete using homogenization concepts. Shi et al. [45] also used Hashin–Shtrikman-based formulations to determine the effective elastic properties of concrete composites.

In the present study, concrete is considered as the matrix phase, while bio-sourced nano-$CaCO_3$ particles are considered as the reinforcing phase. Waste eggshells are adopted as the representative bio-sourced calcium carbonate material. These wastes are rich in calcium carbonate; however, calcium carbonate nanoparticles are not directly present in the raw eggshell waste. Nano-$CaCO_3$ particles can be obtained after suitable processing methods such as cleaning, drying, grinding, calcination, ball milling, or chemical precipitation.

The homogenized material is assumed to be isotropic, linearly elastic, and perfectly bonded. The reinforcement is assumed to be uniformly dispersed in the concrete matrix. The considered reinforcement volume fractions are 10% and 20%. It should be emphasized that the Hashin–Shtrikman model is used here only to estimate the effective macroscopic mechanical properties of the nano-$CaCO_3$-reinforced concrete. It does not describe local nano-scale phenomena such as nanoparticle agglomeration, interfacial transition zones, chemical reactions, imperfect bonding, size-dependent effects, microcracking, damage evolution, or porosity changes. Therefore, the term effective mechanical properties is adopted in this work instead of nano-mechanical characterization.

The following assumptions are adopted in the homogenization procedure: the concrete matrix and nano-$CaCO_3$ reinforcement are isotropic and linearly elastic; the bonding between the matrix and the reinforcement is perfect; the nano-$CaCO_3$ particles are homogeneously dispersed in the concrete matrix; the composite is treated as a two-phase material; and the homogenized material behaves as an equivalent isotropic continuum. Damage, cracking, porosity evolution, and particle agglomeration are not considered.

For a two-phase isotropic composite, the Hashin–Shtrikman bounds are used to estimate the effective bulk modulus and shear modulus of the homogenized concrete. The lower and upper bounds of the effective bulk modulus are expressed as:

$$K^- = K_M + \frac{V_R}{(K_R - K_M)^{-1} + 3(1 - V_R)(K_M + 4G_M)^{-1}} \quad (1)$$

$$K^+ = K_R + \frac{V_M}{(K_M - K_R)^{-1} + 3V_R(K_R + 4G_R)^{-1}} \quad (2)$$

with:

$$K^- \leq K^* \leq K^+$$

where K^- and K^+ are the lower and upper Hashin–Shtrikman bounds of the effective bulk modulus, respectively. K^* is the effective bulk modulus of the homogenized composite. K_M and K_R are the bulk moduli of the concrete matrix and nano-$CaCO_3$ reinforcement, respectivelywhile V_M and $V_R$are their corresponding volume fractions.

Similarly, the lower and upper bounds of the effective shear modulus are given by:

$$G^- = G_M + \frac{V_R}{(G_R - G_M)^{-1} + 6(1 - V_R)(K_M + 2G_M)\left[5G_M(3K_M + 4G_M)\right]^{-1}} \quad (3)$$

$$G^+ = G_R + \frac{V_M}{(G_M - G_R)^{-1} + 6V_R(K_R + 2G_R)\left[5G_R(3K_R + 4G_R)\right]^{-1}} \quad (4)$$

with:

$$G^- \leq G^* \leq G^+ \quad (5)$$

where G^- and G^+ are the lower and upper Hashin–Shtrikman bounds of the effective shear modulus, respectively. $G^*$is the effective shear modulus of the homogenized composite. G_M and G_R are the shear moduli of the concrete matrix and nano-$CaCO_3$ reinforcement, respectively.

In the present work, the effective bulk modulus and shear modulus are taken as the average values of the lower and upper Hashin–Shtrikman bounds:

$$K^* = \frac{K^- + K^+}{2} \quad (6)$$

$$G^* = \frac{G^- + G^+}{2} \quad (7)$$

The effective Young's modulus and Poisson's ratio of the homogenized concrete are then obtained from the classical isotropic elasticity relationships:

$$E^* = \frac{9K^*G^*}{3K^* + G^*} \quad (8)$$

$$\nu^* = \frac{3K^* - 2G^*}{2(3K^* + G^*)} \quad (9)$$

The effective density of the composite is calculated using the rule of mixtures:

$$\rho^* = V_M\rho_M + V_R\rho_R \quad (10)$$

with:

$$V_M + V_R = 1 \quad (11)$$

where ρ^* is the effective density of the homogenized composite, while ρ_M and ρ_R are the densities of the concrete matrix and nano-$CaCO_3$ reinforcement, respectively.The symbols used in the homogenization model are defined as follows:

$K^-$and $K^+$are the lower and upper Hashin–Shtrikman bounds of the bulk modulus;

K^* is the effective bulk modulus of the homogenized composite;

$K_M$and $K_R$are the bulk moduli of the matrix and reinforcement;

$G^-$and G^+ are the lower and upper Hashin–Shtrikman bounds of the shear modulus;

G^* is the effective shear modulus of the homogenized composite;

$G_M$and $G_R$are the shear moduli of the matrix and reinforcement;

$E^*$is the effective Young's modulus of the homogenized composite;

v^* is the effective Poisson's ratio;

$\rho^*$is the effective density;

V_M and V_R are the volume fractions of the matrix and reinforcement, respectively.

2.2. Free vibration formulation of the homogenized simply supported slab

The homogenized effective properties obtained from the Hashin–Shtrikman model are introduced into the free vibration analysis of a simply supported rectangular eco-concrete slab reinforced with bio-sourced nano-$CaCO_3$ particles. The slab has length *a* width *b* and thickness *h*. The effective Young's modulus E^* shear modulus G^*,Poisson's ratio $\nu^*$and density $\rho^*$are used in the structural formulation.

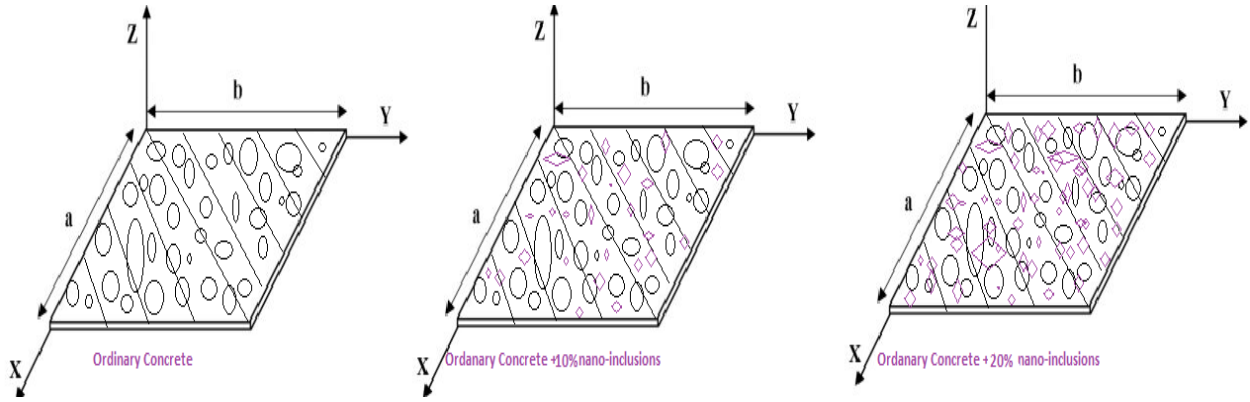

Figure 1. Geometry and simply supported boundary conditions of the rectangular eco-concrete slab reinforced with bio-sourced nano-$CaCO_3$ particles.

The displacement field is defined according to the refined shear deformation plate theory. The displacement components in the ***x, y*** and ***z*** directions are expressed as:

$$u(x,y,z,t) = u_0(x,y,t) - z\frac{\partial w_b}{\partial x} + f(z)\frac{\partial w_s}{\partial x} \quad (11)$$

$$v(x,y,z,t) = v_0(x,y,t) - z\frac{\partial w_b}{\partial y} + f(z)\frac{\partial w_s}{\partial y} \quad (12)$$

$$w(x,y,z,t) = w_b(x,y,t) + w_s(x,y,t) \quad (13)$$

where u_0 and $v_0$are the in-plane displacements of the mid-plane in the *x* and *y* directions, respectively. The functions $w_b$and $w_s$denote the bending and shear components of the transverse displacement, respectively. The function *f(z)* represents the through-thickness shape function adopted in the refined shear deformation theory.

For the first-order shear deformation theory, FSDT, a shear correction factor κ_s is required to correct the non-uniform distribution of transverse shear stresses through the slab thickness. In the present study, κ_s=*5/6* is adopted for the FSDT formulation. However, this factor is not required in the higher-order shear deformation theory, HSDT, because the higher-order displacement field provides a more realistic transverse shear strain distribution. Therefore, $\kappa_s$is used only in the FSDT formulation and must be removed from the HSDT formulation.

For the homogenized isotropic eco-concrete slab, the constitutive stress–strain relationship is written as:

$$\{\sigma\} = [Q]\{\varepsilon\} \quad (15)$$

where [Q] is the elastic stiffness matrix of the homogenized isotropic material. The reduced stiffness coefficients are given by:

$$Q_{11} = Q_{22} = \frac{E^*}{1-(\nu^*)^2},$$

$$Q_{12} = \frac{\nu^* E^*}{1-(\nu^*)^2} \quad (16)$$

$$Q_{44} = Q_{55} = Q_{66} = G^* \quad (17)$$

where E^*, G^*, and ν^* are the effective Young's modulus, shear modulus, and Poisson's ratio of the homogenized eco-concrete, respectively.

The strain components are obtained from the displacement field as follows:

$$\varepsilon_x = \frac{\partial u}{\partial x}, \qquad \varepsilon_y = \frac{\partial v}{\partial y},$$

$$\gamma_{xy} = \frac{\partial u}{\partial y} + \frac{\partial v}{\partial x} \quad (18)$$

$$\gamma_{xz} = \frac{\partial u}{\partial z} + \frac{\partial w}{\partial x}, \qquad \gamma_{yz} = \frac{\partial v}{\partial z} + \frac{\partial w}{\partial y} \tag{19}$$

For free vibration analysis, no external mechanical load and no thermal load are applied. Therefore, the virtual external work is equal to zero:

$$\delta V = 0 \tag{20}$$

The governing equations are derived using the principle of virtual work, or equivalently Hamilton's principle, as:

$$\int_{t_1}^{t_2} (\delta U - \delta T)\, dt = 0 \tag{21}$$

where δU is the virtual strain energy and δT is the virtual kinetic energy. The virtual strain energy of the slab is expressed as:

$$\delta U = \int_V (\sigma_x \delta\varepsilon_x + \sigma_y \delta\varepsilon_y + \tau_{xy}\delta\gamma_{xy} + \tau_{xz}\delta\gamma_{xz} + \tau_{yz}\delta\gamma_{yz})\, dV \tag{22}$$

The kinetic energy is written as:

$$T = \frac{1}{2}\int_V \rho^* \left(\dot{u}^2 + \dot{v}^2 + \dot{w}^2\right) dV \tag{23}$$

where ρ^* is the effective density of the homogenized eco-concrete, and the dot denotes differentiation with respect to time.

The variation of the kinetic energy is therefore given by:

$$\delta T = \int_V \rho^* (\dot{u}\delta\dot{u} + \dot{v}\delta\dot{v} + \dot{w}\delta\dot{w})\, dV \tag{23a}$$

By integrating Eq. (23a) by parts with respect to time, and assuming that the virtual displacements vanish at the time boundaries t_1 and t_2, one obtains:

$$\int_{t_1}^{t_2} \delta T\, dt = -\int_{t_1}^{t_2}\int_V \rho^* (\ddot{u}\delta u + \ddot{v}\delta v + \ddot{w}\delta w)\, dV\, dt \tag{23b}$$

Thus, the dynamic effect appears explicitly through the inertia terms:

$$\rho^*\ddot{u}, \qquad \rho^*\ddot{v}, \qquad \rho^*\ddot{w} \tag{23c}$$

These terms represent the resistance of the slab to acceleration and lead directly to the formation of the mass matrix in the final free vibration problem.

By substituting the displacement field given in Eqs. (11)-(13) into the kinetic energy expression, the velocity components are obtained as:

$$\dot{u} = \dot{u}_0 - z\frac{\partial \dot{w}_b}{\partial x} - f(z)\frac{\partial \dot{w}_s}{\partial x} \tag{23d}$$

$$\dot{v} = \dot{v}_0 - z\frac{\partial \dot{w}_b}{\partial y} - f(z)\frac{\partial \dot{w}_s}{\partial y} \tag{23e}$$

$$\dot{w} = \dot{w}_b + \dot{w}_s \tag{23f}$$

Therefore, the kinetic energy includes the inertia effects associated with the in-plane displacements, the bending transverse displacement, the shear transverse displacement, and the coupling terms between these variables. Consequently, the mass matrix depends on the effective density ρ^*, the slab thickness h, and the adopted through-thickness shear function ***f(z)***.

The stress resultants and moment resultants are defined as:

$$N_{ij} = \int_{-h/2}^{h/2} \sigma_{ij}\, dz \tag{24a}$$

$$M_{ij}^b = \int_{-h/2}^{h/2} z\sigma_{ij}\, dz \tag{24b}$$

$$M_{ij}^s = \int_{-h/2}^{h/2} f(z)\sigma_{ij}\, dz \tag{24c}$$

$$Q_{ij} = \int_{-h/2}^{h/2} g(z)\tau_{ij}\, dz \tag{24d}$$

Where *I ,j=x,y*. Here, N_{ij} denotes the membrane force resultants, M_{ijb} and M_{ijs} are the bending and shear-related moment resultants, and Q_{ij}denotes the transverse shear force resultants.The function *g(z)* is associated with the transverse shear strain

distribution and is generally related to *1−f′(z)*.

The inertia coefficients may also be introduced by integrating the density terms through the thickness as follows:

$$I_0 = \int_{-h/2}^{h/2} \rho^* \, dz \tag{24e}$$

$$I_1 = \int_{-h/2}^{h/2} \rho^* z \, dz \tag{24f}$$

$$I_2 = \int_{-h/2}^{h/2} \rho^* z^2 \, dz \tag{24g}$$

$$J_1 = \int_{-h/2}^{h/2} \rho^* f(z) \, dz \tag{24h}$$

$$J_2 = \int_{-h/2}^{h/2} \rho^* z f(z) \, dz \tag{24i}$$

$$K_2 = \int_{-h/2}^{h/2} \rho^* f^2(z) \, dz \tag{24j}$$

These inertia coefficients contribute to the construction of the mass matrix *[M].* For a homogeneous effective density ρ^*, they depend only on the slab thickness and the selected thickness function *f(z).*

By substituting the displacement field, strain components, constitutive relations, and stress resultants into Hamilton's principle, and by performing integration by parts while collecting the coefficients of the virtual displacement variations δu_0, δv_0, δw_b and δw_s, the governing equations of free vibration are obtained in terms of the generalized displacement variables. Since the present study is limited to free vibration, no mechanical bending loads or thermal loads are included in these governing equations.

For a simply supported rectangular slab, the boundary conditions are defined as follows:

*At **x=0** and **x=a**:*

$$v_0 = 0, \qquad w_b = 0, \qquad w_s = 0,$$
$$N_x = 0, \qquad M_x^b = 0, \qquad M_x^s = 0 \tag{25a}$$

At ***y=0*** and ***y=b***:

$$u_0 = 0, \qquad w_b = 0, \qquad w_s = 0,$$
$$N_y = 0, \qquad M_y^b = 0, \qquad M_y^s = 0 \tag{25b}$$

The Navier solution is then adopted because it satisfies the simply supported boundary conditions. The admissible displacement functions are expressed as:

$$u_0(x,y,t) = \sum_{m=1}^{\infty}\sum_{n=1}^{\infty} U_{mn} \cos(\alpha x) \sin(\beta y) e^{i\omega t} \tag{26}$$

$$v_0(x,y,t) = \sum_{m=1}^{\infty}\sum_{n=1}^{\infty} V_{mn} \sin(\alpha x) \cos(\beta y) e^{i\omega t} \tag{27}$$

$$w_b(x,y,t) = \sum_{m=1}^{\infty}\sum_{n=1}^{\infty} W_{bmn} \sin(\alpha x) \sin(\beta y) e^{i\omega t} \tag{28}$$

$$w_s(x,y,t) = \sum_{m=1}^{\infty}\sum_{n=1}^{\infty} W_{smn} \sin(\alpha x) \sin(\beta y) e^{i\omega t} \tag{29}$$

where U_{mn}, V_{mn}, W_{bmn}, and W_{smn} are the unknown displacement amplitudes. The wave numbers α and β are defined as:

$$\alpha = \frac{m\pi}{a}, \qquad \beta = \frac{n\pi}{b} \tag{30}$$

where *m* and *n* are the half-wave numbers in the *x* and *y* directions, respectively.

After substituting Navier's admissible displacement functions into the governing equations, the spatial derivatives are transformed into algebraic terms involving α and β. Moreover, for harmonic motion, the second-order time derivative gives:

$$\ddot{\Delta} = -\omega^2 \Delta \tag{30a}$$

Consequently, the free vibration problem is written in matrix form as:

$$\left([K] - \omega^2 [M]\right) \{\Delta\} = 0 \tag{31}$$

where ***[K]*** is the stiffness matrix, ***[M]*** is the mass matrix, and ***{Δ}*** is the vector of unknown displacement amplitudes:

$$\{\Delta\} = \{U_{mn}, V_{mn}, W_{bmn}, W_{smn}\}^T \tag{32}$$

For non-trivial solutions, the determinant of the dynamic stiffness matrix must vanish:

$$\det\left([K]-\omega^2[M]\right)=0 \tag{33}$$

Equation (33) represents the eigenvalue problem of the free vibration analysis. Solving this equation gives the natural circular frequencies ***ω*** of the simply supported eco-concrete slab.

To avoid confusion in notation, the following convention is adopted throughout the manuscript: *w* denotes the transverse displacement, *ω* denotes the natural circular frequency, and *Ω* denotes the dimensionless natural frequency parameter. Therefore, the symbol *N* is not used to denote the frequency parameter, because N_{ij} is already used for the membrane force resultants.

The dimensionless natural frequency parameter is defined as:

$$\Omega=\omega h\sqrt{\frac{\rho^*}{G^*}} \tag{34}$$

Alternatively, for comparison with some reference solutions, the following normalized frequency parameter may be used:

$$\Omega=\omega\frac{a^2}{h}\sqrt{\frac{\rho^*}{E^*}} \tag{35}$$

Only one definition of ***Ω*** must be retained consistently throughout the manuscript, depending on the normalization adopted in the validation study.

The functions used for the First-Order Shear Deformation Theory (FSDT):

$$f(z)=z,\qquad g(z)=\frac{\partial f(z)}{\partial z},\qquad k_s=\frac{5}{6} \tag{36}$$

The functions used for the Higher-Order Shear Deformation Theory (HSDT).

$$f(z)=z\left(1-\frac{4z^2}{3h^2}\right),\qquad g(z)=\frac{\partial f(z)}{\partial z},\qquad k_s=1 \tag{37}$$

4. RESULTS AND DISCUSSION

The present section discusses the effective mechanical properties and the free vibration response of simply supported eco-concrete slabs reinforced with bio-sourced nano-$CaCO_3$ particles. The results are presented in three main parts. First, the mechanical properties of the constituent materials are reported. Second, the effective properties obtained from different homogenization models are compared. Finally, the free vibration response of ordinary concrete slabs and nano-$CaCO_3$-reinforced concrete slabs is analyzed.

The notation used in this section is unified as follows: w denotes the transverse displacement, ω denotes the natural circular frequency, and Ω denotes the dimensionless natural frequency parameter. Therefore, all vibration results are discussed in terms of the dimensionless natural frequency Ω.

Table 1 summarizes the mechanical properties of the constituent materials used in this study. Ordinary concrete is considered as the matrix phase, while bio-sourced nano-$CaCO_3$ particles are considered as the reinforcing phase. The material properties are adopted from the literature.

Table 1. Mechanical properties of the constituent materials used before homogenization.

Property	**Symbol**	**Concrete matrix**	**Symbol**	**Nano-$CaCO_3$ reinforcement**
Young's modulus	EM (GPa)	20	ER (GPa)	68.7
Poisson's ratio	vM	0.3	vR	0.329
Shear modulus	GM (GPa)	7.79	GR (GPa)	25.82
Bulk modulus	KM (GPa)	16.67	KR (GPa)	67.08
Density	ρM (kg/m³)	2500	ρR (kg/m³)	2620

The first theoretical approaches for the homogenization of composite materials were introduced by Voigt, who assumed uniform strain in all phases of the material. Reuss later proposed a model based on uniform stress, which generally provides a lower estimate of the effective properties. Eshelby developed a fundamental solution for an ellipsoidal inclusion embedded in an infinite matrix, which became the basis for several micromechanical models. Hashin and Shtrikman established rigorous upper and lower bounds for the effective properties of isotropic multiphase composites. Mori and Tanaka later proposed a homogenization model based on Eshelby's inclusion theory for composites containing dispersed inclusions.

In this study, the effective properties of concrete reinforced with 10% and 20% nano-$CaCO_3$ are estimated using different homogenization approaches. The comparison is given in Table 2.

Table 2. Comparison of effective mechanical properties predicted by different homogenization models.

Model	E* (GPa)	ν^*	G* (GPa)	K^* (GPa)	E* (GPa)	ν^*	G* (GPa)	K^* (GPa)
V_w	10%				20%			
Voigt	24.87	0.300	9.57	20.73	29.74	0.300	11.44	24.78
Reuss	22.25	0.300	8.54	18.52	24.32	0.300	9.62	20.83
Eshelby	22.20	0.302	8.53	18.58	24.40	0.304	9.65	20.98
Mori–Tanaka	22.34	0.303	8.60	18.72	24.97	0.306	9.86	21.52
HS−	22.33	0.303	8.60	18.72	24.95	0.306	9.86	21.52
HS+	23.28	0.301	8.96	19.52	26.81	0.303	10.53	23.10
HS ^{M}	22.81	0.302	8.78	19.12	25.88	0.305	10.20	22.31

Table 2 shows that the Hashin–Shtrikman mean values are located between the lower and upper bounds, as expected. For a 10% nano-$CaCO_3$ volume fraction, the effective Young's modulus obtained using the Hashin–Shtrikman mean value is 22.81 GPa. For a 20% nano-$CaCO_3$ volume fraction, it increases to 25.88 GPa. These values are consistent with the predictions of the Eshelby and Mori–Tanaka approaches, which confirms that the Hashin–Shtrikman model provides a suitable estimation of the effective macroscopic properties of the reinforced concrete.

The effective properties retained for the vibration analysis are summarized in Table 3. Ordinary concrete is also included for comparison.

Table 3. Effective mechanical properties of ordinary concrete and nano-$CaCO_3$-reinforced concrete.

Properties	Elastic modulus	Poisson's ratio	Shear modulus	Bulk modulus	Density
Symbols and Units	E* (GPa)	ν^*	G* (GPa)	K^* (GPa)	ρ^* (Kg/m^3)
V_w(0%)	20	0.3	7.69	16.67	2500
V_w(10%)	22.81	0.302	8.78	19.12	2506
V_w(20%)	25.88	0.305	10.20	22.31	2512

The results in Table 3 show that the incorporation of nano-$CaCO_3$ improves the effective mechanical properties of concrete. Compared with ordinary concrete, the Young's modulus increases from 20.00 GPa to 22.81 GPa for 10% reinforcement, corresponding to an improvement of approximately 14.05%. For 20% reinforcement, the Young's modulus reaches 25.88 GPa, corresponding to an improvement of approximately 29.40%. The shear modulus increases from 7.69 GPa to 8.78 GPa and 10.20 GPa for 10% and 20% nano-$CaCO_3$, respectively. The bulk modulus also increases from 16.67 GPa to 19.12 GPa and 22.31 GPa. The density increases only slightly because the density of nano-$CaCO_3$ is close to that of ordinary concrete. These results confirm that nano-$CaCO_3$ reinforcement mainly improves the stiffness of the homogenized concrete composite.

Before performing the parametric vibration analysis, the present formulation is validated by comparison with reference results reported by Ghugal and Sayyad [49]. The comparison is carried out for square and rectangular simply supported isotropic plates with a/h=10. The results are presented in Table 4.

Table 4. Validation of the present FSDT and HSDT results against the reference solution of Ghugal and Sayyad [49] for simply supported isotropic plates with a/h=10.

frequencies	Ω					
Shape of plate	**Square**			**Rectangular**		
Modes/Methods	Ghugal and Sayyad [49]	Present (FSDT)	Present (HSDT)	Ghugal and Sayyad [49]	Present (FSDT)	Present (HSDT)
(1,1)	0.0933	0.0944	0.0921	0.0705	0.0702	0.0690
(1,2)	0.2231	0.2361	0.2222	0.1393	0.1405	0.1356
(1,3)	0.4148	0.4721	0.4201	0.2438	0.2576	0.2416

The comparison in Table 4 shows that the present results are in good agreement with the reference solution. The HSDT results are generally closer to the reference values than the FSDT results. For example, for the square plate in mode (1,2), the reference value is 0.2231, while the present HSDT result is 0.2222. For the rectangular plate in mode (1,3), the reference value is 0.2438, while the present HSDT result is 0.2416. These comparisons confirm the accuracy of the present formulation. Therefore, HSDT is adopted in the following parametric analysis because it provides better agreement with the reference results and does not require a shear correction factor.

Table 5 presents the effect of nano-$CaCO_3$ reinforcement on the dimensionless natural frequencies of square and rectangular simply supported slabs. The comparison is carried out for ordinary concrete and concrete reinforced with 10% and 20% nano-$CaCO_3$.

Table 5.Dimensionless natural frequencies Ω of ordinary and nano-$CaCO_3$-reinforced simply supported concrete slabs.

frequencies	**Ω**					
Shape of plate	**Square**			**Rectangular**		
Modes/Vf	0%	10%	20%	0%	10%	20%
(1,1)	0.0921	0.1277	0.1287	0.0690	0.0956	0.0965
(1,2)	0.2222	0.3078	0.3104	0.1356	0.1879	0.1895
(1,3)	0.4206	0.5821	0.5868	0.2416	0.3347	0.3375

The results in Table 5 show that the addition of nano-$CaCO_3$ significantly increases the dimensionless natural frequencies of the concrete slabs. For the square plate in the fundamental mode (1,1), the frequency increases from 0.0921 for ordinary concrete to 0.1277 for 10% nano-$CaCO_3$ and 0.1287 for 20% nano-$CaCO_3$. These values correspond to increases of approximately 38.65% and 39.74%, respectively. For the rectangular plate in the fundamental mode, the frequency increases from 0.0690 to 0.0956 and 0.0965, corresponding to increases of approximately 38.55% and 39.86%, respectively.

Although the 20% reinforcement case gives the highest frequency values, the improvement between 10% and 20% nano-$CaCO_3$ is very limited. For the square plate in mode (1,1), the increase from 10% to 20% is only about 0.78%. For the rectangular plate in the same mode, the increase is about 0.94%. This indicates that 10% nano-$CaCO_3$ provides most of the vibration improvement, while increasing the reinforcement content to 20% gives only a marginal additional benefit. Therefore, 10% nano-$CaCO_3$ may be considered an efficient reinforcement content from both mechanical and economic viewpoints.

The increase in natural frequency is mainly attributed to the increase in the effective stiffness of the homogenized concrete composite. Since the density increases only slightly with the addition of nano-$CaCO_3$, the stiffness improvement dominates the dynamic response. Consequently, the reinforced slabs exhibit higher natural frequencies than ordinary concrete slabs.The figure captions are revised as follows to improve clarity and consistency.

Figures 2 and 3 show the influence of the length-to-thickness ratio a/h on the dimensionless natural frequency Ω of square simply supported slabs. As a/h increases, the dimensionless natural frequency decreases. This trend is physically expected because increasing a/h corresponds to a relatively thinner slab, which reduces the bending stiffness and consequently decreases the vibration frequency. For both vibration modes, the reinforced slabs show higher frequencies than ordinary concrete slabs. The mode (m=n=2) gives higher frequency values than the fundamental mode (m=n=1), which is consistent with classical plate vibration behavior.

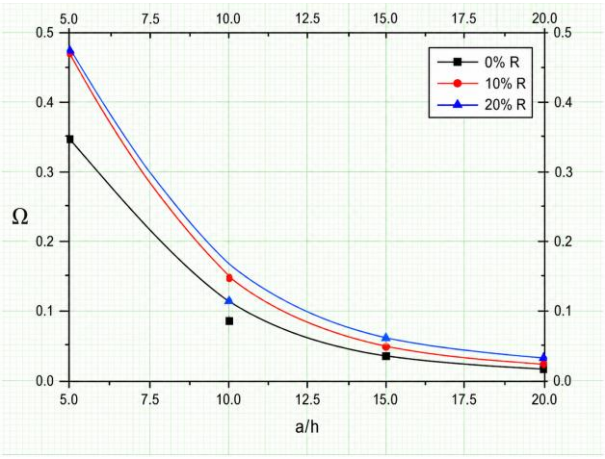

Figure 2. Variation of the dimensionless natural frequency Ω with the length-to-thickness ratio a/h for a square simply supported slab, considering the fundamental mode (m=n=1) and different nano-$CaCO_3$ volume fractions

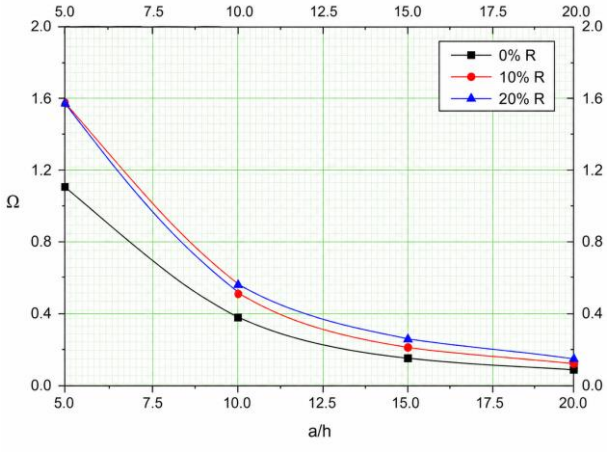

Figure 3. Variation of the dimensionless natural frequency Ω with the length-to-thickness ratio a/h for a square simply supported slab, considering the vibration mode (m=n=2) and different nano-$CaCO_3$ volume fractions

Figures 4 and 5 show the influence of the aspect ratio b/a on the dimensionless natural frequency Ω of rectangular simply supported slabs. The results indicate that the frequency decreases as b/a increases. This behavior is related to the increase in the effective plate dimension, which reduces the relative structural stiffness. As observed in Figures 2 and 3, the addition of nano-$CaCO_3$ increases the natural frequency for all considered geometrical configurations. However, the difference between 10% and 20% reinforcement remains small, confirming that 10% nano-$CaCO_3$ is an efficient reinforcement fraction for improving the vibration performance of eco-concrete slabs.

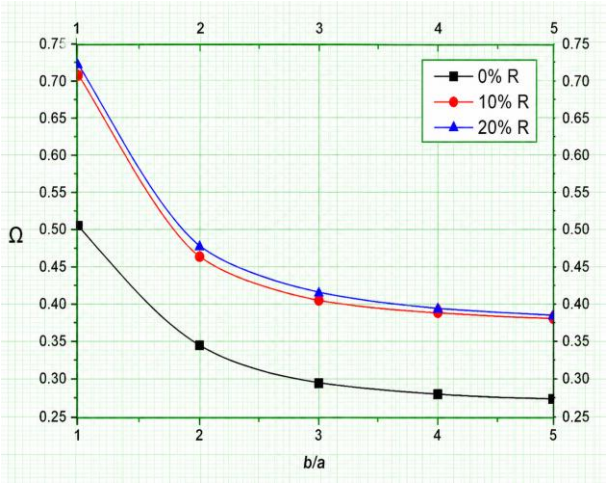

Figure 4. Variation of the dimensionless natural frequency Ω with the aspect ratio b/a for a simply supported rectangular slab with a/h=4, considering the mode (m=n=1) and different nano-$CaCO_3$ volume fractions

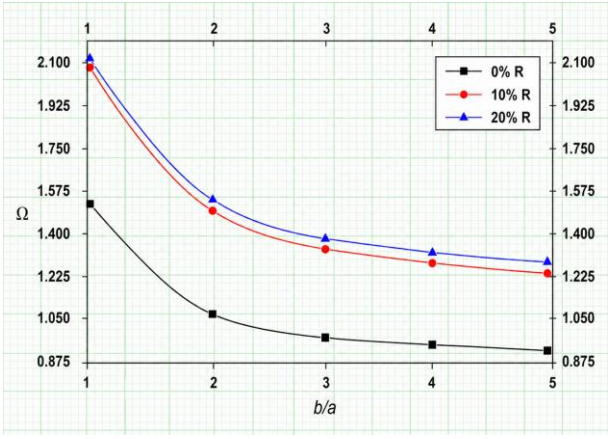

Figure 5. Variation of the dimensionless natural frequency Ω with the aspect ratio b/a for a simply supported rectangular slab with a/h=4, considering the mode (m=n=2) and different nano-$CaCO_3$ volume fractions

Overall, the results demonstrate that bio-sourced nano-$CaCO_3$ reinforcement improves the effective stiffness and dynamic performance of concrete slabs. The Hashin–Shtrikman homogenization model provides effective properties that can be successfully introduced into the HSDT-based free vibration formulation. The results also show that the improvement becomes marginal beyond 10% nano-$CaCO_3$, suggesting that this content represents a suitable compromise between mechanical performance and material economy.

5. CONCLUSION

In this study, the effective mechanical properties and free vibration response of simply supported eco-concrete slabs reinforced with bio-sourced nano-$CaCO_3$ particles were investigated. The effective properties of the reinforced concrete were estimated using the Hashin–Shtrikman homogenization model, while the free vibration behavior of the slabs was analyzed using FSDT and HSDT formulations. Based on the obtained results, the following conclusions can be drawn:

- The Hashin–Shtrikman model provides a suitable analytical framework for estimating the effective macroscopic mechanical properties of concrete reinforced with nano-$CaCO_3$ particles, under the assumptions of perfect bonding, homogeneous dispersion, isotropic behavior, and linear elasticity.
- The incorporation of nano-$CaCO_3$ particles improves the effective stiffness of concrete. The Young's modulus increases from 20.00 GPa for ordinary concrete to 22.81 GPa and 25.88 GPa for 10% and 20% nano-$CaCO_3$ reinforcement, respectively. These values correspond to increases of approximately 14.05% and 29.40%.

- The shear modulus and bulk modulus also increase with nano-$CaCO_3$ content. The shear modulus increases from 7.69 GPa to 8.78 GPa and 10.20 GPa, while the bulk modulus increases from 16.67 GPa to 19.12 GPa and 22.31 GPa for 10% and 20% reinforcement, respectively.
- The free vibration results show that nano-$CaCO_3$ reinforcement increases the dimensionless natural frequencies of simply supported concrete slabs. For the square slab in the fundamental mode (m=n=1), the frequency increases from 0.0921 for ordinary concrete to 0.1277 for 10% nano-$CaCO_3$ and 0.1287 for 20% nano-$CaCO_3$.
- Although the 20% reinforcement case gives the highest stiffness and frequency values, the additional improvement compared with the 10% case is limited. For example, in the square slab fundamental mode, the frequency increases by only about 0.78% when the nano-$CaCO_3$ content increases from 10% to 20%. Therefore, 10% nano-$CaCO_3$ can be considered an efficient reinforcement content from both mechanical and economic viewpoints.
- The comparison with reference results confirms that HSDT gives more accurate frequency predictions than FSDT. In addition, HSDT does not require a shear correction factor, which makes it more suitable for the free vibration analysis of moderately thick eco-concrete slabs.
- The proposed analytical approach provides a useful framework for linking bio-sourced nano-$CaCO_3$ reinforcement, effective stiffness improvement, and free vibration performance of simply supported eco-concrete slabs.

Future research should focus on the following directions:

- Experimental validation of the effective mechanical properties predicted by the Hashin–Shtrikman model using concrete specimens reinforced with bio-sourced nano-$CaCO_3$ particles.
- Investigation of the influence of nanoparticle dispersion, agglomeration, and interfacial bonding on the mechanical and dynamic behavior of nano-$CaCO_3$-reinforced eco-concrete.
- Extension of the present analytical model to include porosity, cracking, damage evolution, and imperfect interfaces between the cement matrix and the nano-$CaCO_3$ particles.
- Analysis of forced vibration, seismic response, and dynamic stability of eco-concrete slabs reinforced with bio-sourced nano-$CaCO_3$ particles.
- Comparison between different bio-sourced calcium carbonate wastes, such as eggshells, fish bones, animal bones, and shells, in terms of mechanical performance, processing requirements, environmental impact, and economic feasibility.
- Development of numerical finite element models and experimental modal tests to validate and extend the present analytical predictions.

Acknowledgement

The project presented in this article is supported by the laboratory of advanced structures and materials in civil engineering and public works, Sidi Bel-Abbes, Algeria.

This research is included in the axes of the Thematic Agency for Research in Science and Technology (ATRST), 16000 Algiers, Algeria.

6. REFERENCES

[1] Z.R. Harrat, S. Amziane, B. Krour, M.B. Bouiadjra (2021) On the static behavior of nano SiO_2 based concrete beams resting on an elastic foundation, Computers and Concrete, 27(6), 575–583. https://doi.org/10.12989/cac.2021.27.6.575

[2] M. Chatbi, B. Krour, M.A. Benatta, Z.R. Harrat, S. Amziane, M.B. Bouiadjra (2022) Bending analysis of nano-SiO_2 reinforced concrete raft foundation resting on elastic foundation, Structural Engineering and Mechanics, 84(5), 685–697. https://doi.org/10.12989/sem.2022.84.5.685

[3] A. Benfrid, A. Benbakhti, Z.R. Harrat, M. Chatbi, B. Krour, M.B. Bouiadjra (2023) Thermomechanical analysis of glass powder based eco-concrete panels: Limitations and performance evaluation, Periodica Polytechnica Civil Engineering, 67(4), 1284–1297. https://doi.org/10.3311/PPci.22781

[4] S.D. Elhennani, Z.R. Harrat, M. Chatbi, A. Belbachir, B. Krour, E. Işık, E. Harirchian, M. Bouremana, M.B. Bouiadjra (2023) Buckling and free vibration analyses of various nanoparticle reinforced concrete beams resting on multi-parameter elastic foundations, Materials, 16(17), 5865. https://doi.org/10.3390/ma16175865

[5] A. Kecir, M. Chatbi, Z.R. Harrat, M.B. Bouiadjra, M. Bouremana, B. Krour (2024) Enhancing the mechanical performance of concrete raft foundation through the incorporation of nano-sized iron oxide particles (Fe_2O_3): Non-local bending analysis, Periodica Polytechnica Civil Engineering, 68(3), 842–858. https://doi.org/10.3311/PPci.23016

[6] H.Y. Jaramillo, O.H. Vasco-Echeverri, L.A. Moreno-Pacheco, R.A. García-León (2023) Biomaterials in concrete for engineering applications: A bibliometric review, Infrastructures, 8(11), 161. https://doi.org/10.3390/infrastructures8110161

[7] W. Schmidt, N.S. Msinjili, S. Pirskawetz, H.C. Kühne (2015) Efficiency of high performance concrete types incorporating bio-materials like rice husk ashes, cassava starch, lignosulfonate, and

sisal fibres, Academic Journal of Civil Engineering, 33(2), 208–214. https://doi.org/10.26168/icbbm2015.32

[8] K. Kawaai, T. Nishida, A. Saito, T. Hayashi (2022) Application de matériaux biosourcés aux méthodes de réparation des fissures et des patchs dans le béton, Construction and Building Materials, 340, 127718. https://doi.org/10.1016/j.conbuildmat.2022.127718

[9] F. Fatahillah, A. Sumarno (2022) The effect of concrete mixture on usage fly ash and chicken egg shell powder as cement substitutions in concrete compressive strength, Neutron, 22(1), 24–30. https://doi.org/10.29138/neutron.v22i01.173

[10] O. Zaid, S.R.Z. Hashmi, M.H. El Ouni, R. Martínez-García, J. de Prado-Gil, S.E.A.S. Yousef (2023) Experimental and analytical study of ultra-high-performance fiber-reinforced concrete modified with egg shell powder and nano-silica, Journal of Materials Research and Technology, 24, 7162–7188. https://doi.org/10.1016/j.jmrt.2023.04.240

[11] E.M. Shcherban', S.A. Stel'makh, A.N. Beskopylny, L.R. Mailyan, B. Meskhi, V. Varavka, N. Beskopylny, D. El'shaeva (2022) Enhanced eco-friendly concrete nano-change with eggshell powder, Applied Sciences, 12(13), 6606. https://doi.org/10.3390/app12136606

[12] J. Bhat, R.A. Qasab, A.R. Dar (2012) Machine crushed animal bones as partial replacement of coarse aggregates in lightweight concrete, ARPN Journal of Engineering and Applied Sciences, 7(9), 1202–1207.

[13] K. Claudius, A.S. Baba, A. Abubakar (2023) Influence of pulverized animal bone and animal bone ash on the mechanical properties of normal strength concrete using response surface method, Construction, 3(1), 63–74. https://doi.org/10.15282/construction.v3i1.9097

[14] S. Damayanti, T.B. Aulia, Y. Hayati (2020) The effect of fishbone fiber and rice husk ash additive on the mechanical properties of normal concrete, IOP Conference Series: Materials Science and Engineering, 933, 012036. https://doi.org/10.1088/1757-899X/933/1/012036

[15] F.A. Arain, M.A. Jatoi, M.S. Raza, F.A. Shaikh, F. Khowaja, K. Rai (2022) Preliminary investigation on properties of novel sustainable composite: Fish scales reinforced cement concrete, Jurnal Kejuruteraan, 34(2), 309–315. https://doi.org/10.17576/jkukm-2022-34(2)-14

[16] E.A. Sulaiman, J.J.H. Alwash, T.A. Jasim, Z. Al-Khafaji, M. Falah, S.S.A.O. Al-Edrus (2025) Investigating the effect of applying fish scale powder in concrete as sustainable blending materials, Review of Composite Materials and Applications, 35(3), 403–412. https://doi.org/10.18280/rcma.350302

[17] T. Higashino, A. Yanaka, Y. Oyake, S. Okazaki, Y. Suenaga, H. Yoshida (2025) Development of a porous concrete mixed with hydroxyapatite produced from fish bones, GEOMATE Journal, 28(130), 112–122. https://geomatejournal.com/geomate/article/view/5068

[18] A. Yanaka, H. Yoshida, S. Okazaki, Y. Oyake, Y. Suenaga (2023) Recycling of fishery waste as planting base porous concrete aimed at achieving carbon neutrality, GEOMATE Journal, 24(104), 85–92. https://geomatejournal.com/geomate/article/view/3845

[19] H. Ding, W. Chen, R. Xu (2001) On the bending, vibration and stability of laminated rectangular plates with transversely isotropic layers, Applied Mathematics and Mechanics, 22(1), 17–24.

[20] M. Alfano, L. Pagnotta (2006) Determining the elastic constants of isotropic materials by modal vibration testing of rectangular thin plates, Journal of Sound and Vibration, 293, 426–439. https://doi.org/10.1016/j.jsv.2005.10.021

[21] F. Turan (2025) Natural frequencies of shear deformable porous orthotropic laminated doubly-curved shallow shells with non-uniformly distributed porosity using higher-order shear deformation theory, Thin-Walled Structures, 210, 112951. https://doi.org/10.1016/j.tws.2025.112951

[22] F. Turan, M. Karadeniz, E. Zeren (2024) Free vibration and buckling behavior of porous orthotropic doubly-curved shallow shells subjected to non-uniform edge compression using higher-order shear deformation theory, Thin-Walled Structures, 205, 112522. https://doi.org/10.1016/j.tws.2024.112522

[23] F. Turan (2024) Free vibration response of multi-layered plates with trigonometrically distributed porosity based on the higher-order shear deformation theory, Steel and Composite Structures, 53(1), 77–90. https://doi.org/10.12989/scs.2024.53.1.077

[24] F.C. Bahadır, F. Turan (2024) On the vibration responses of orthotropic laminated cylindrical panels with non-uniform porosity distributions using higher-order shear deformation theory, Mechanics Based Design of Structures and Machines, 52(12), 9975–10005. https://doi.org/10.1080/15397734.2024.2352585

[25] F. Turan (2023) Vibration analysis of porous orthotropic cylindrical panels resting on elastic foundations based on shear deformation theory, International Journal of Engineering and Applied Sciences, 15(3), 125–143. https://doi.org/10.24107/ijeas.1342775

[26] F. Turan (2023) Natural frequencies of porous orthotropic two-layered plates within the shear deformation theory, Challenge Journal of Structural Mechanics. https://doi.org/10.20528/cjsmec.2023.01.001

[27] A. Doicheva, K. Mladenov (2005) On some dynamic characteristics in the analysis of building structures, Scientific Conference with International Participation, Stara Zagora, Bulgaria, proceedings, 1, 139–145.

[28] V. Rizov, A. Doicheva, A. Mladensky, G. Keradjiyski (2015) Analysis of a pedestrian bridge with respect to the comfort using the Eurocode, Annual of the University of Architecture, Civil Engineering and Geodesy, XLVIII(VIII-B), 79–89.

[29] E. Işık (2025) A study on strengthening RC structural elements with fibers based polymers, Bitlis Eren University Journal of Science, 14(2), 1269–1286. https://doi.org/10.17798/bitlisfen.1675489

[30] C. Ike (2025) Ritz variational method for the free harmonic vibration solutions of slender beams on two-parameter elastic foundations, Nigerian Journal of Technology, 44(2), 193–201. https://doi.org/10.4314/njt.v44i2.3

[31] C. Ike (2025) Solving lateral-torsional buckling problems in thin-walled bisymmetric beam using Stodola-Vianelo iteration method, Nigerian Journal of Technology, 44(1), 1–8. https://doi.org/10.4314/njt.v44i1.1

[32] C. Ike (2024) Stodola-Vianelo iteration method for solving transverse harmonic natural vibration problems of Euler-Bernoulli beams on Winkler foundations, Iraqi Journal of Civil Engineering, 18(2), 73–87. https://doi.org/10.37650/ijce.2024.180206

[33] N. Lecompte, A. Caratenuto, Y. Zheng (2025) Waste animal bone-derived calcium phosphate particles with high solar reflectance, arXiv preprint. https://doi.org/10.48550/arXiv.2501.18130

[34] S.K. Tiwari, M. Bystrzejewski, A.D. Adhikari, A. Huczko, N. Wang (2022) Methods for the conversion of biomass waste into value-added carbon nanomaterials: Recent progress and applications, Progress in Energy and Combustion Science, 92, 101023. https://doi.org/10.1016/j.pecs.2022.101023

[35] M.H. Hussin, N.H. Abd Latif, T.S. Hamidon, N.N. Idris, R. Hashim, J.N. Appaturi, N. Brosse, I. Ziegler-Devin, L. Chrusiel, W. Fatriasari, F.A. Syamani, A.H. Iswanto, L.S. Hua, S.S.A. Osman Al Edrus, W.C. Lum, P. Antov, V. Savov, M.A.R. Lubis, L. Kristak, R. Reh, J. Sedliačik (2022) Latest advancements in high-performance bio-based wood adhesives: A critical review, Journal of Materials Research and Technology, 21, 3909–3946. https://doi.org/10.1016/j.jmrt.2022.10.156

[36] Z. Hashin, S. Shtrikman (1963) A variational approach to the theory of elastic behaviour of multiphase materials, Journal of the Mechanics and Physics of Solids, 11, 127–140. https://doi.org/10.1016/0022-5096(63)90060-7

[37] C. Shi, Q. Tu, H. Fan, S. Li (2016) An interphase model for effective elastic properties of concrete composites, Journal of Micromechanics and Molecular Physics, 1(1), 1650005. https://doi.org/10.1142/S2424913016500053

[38] Z. Dong, W. Quan, X. Ma, X. Li, J. Zhou (2023) Asymptotic homogenization of effective thermal-elastic properties of concrete considering its three-dimensional mesostructure, Computers & Structures, 279, 106970. https://doi.org/10.1016/j.compstruc.2022.106970

[39] P. Wall (1997) A comparison of homogenization, Hashin–Shtrikman bounds and the Halpin–Tsai equations, Applications of Mathematics, 42(4), 245–257.

[40] S. Kurukuri (2005) Homogenization of damaged concrete meso-structures using representative volume elements – Implementation and application to SLang, Master's thesis, Bauhaus–University Weimar, Weimar, Germany.

[41] A. Benfrid, K. Murawski (2025) Thermo-mechanics of eco-concrete beams reinforced with waste pottery, International Science and Technology Journal, 37(2), 1–23. https://doi.org/10.62341/AKBM2379

[42] T.-F.F. Lee, M.D. Cohen (n.d.) Strength and durability of concrete: Effects of cement paste-aggregate interfaces, Part II: Significance of transition zones on physical and mechanical properties of Portland cement mortar, JTRP Technical Report.

[43] R. Luciano, J.R. Willis (2006) Hashin–Shtrikman based FE analysis of the elastic behaviour of finite random composite bodies, International Journal of Fracture, 137, 261–273. https://doi.org/10.1007/s10704-005-3067-z

[44] F. Aouissi, C.-C. Yang, A. Brahma, O. Zorkane (2018) Comparison between biphasic and triphasic model for predicting the elastic modulus of concrete, MATEC Web of Conferences, 203, 06003. https://doi.org/10.1051/matecconf/201820306003

[45] C. Shi, Q. Tu, H. Fan, S. Li (2016) Micromechanical modeling of effective elastic properties of concrete considering interphase effects, Journal of Micromechanics and Molecular Physics, 1(1), 1650005. https://doi.org/10.1142/S2424913016500053

[46] P.V. Avhad, A.S. Sayyad (2020) On the static deformation of FG sandwich beams curved in elevation using a new higher order beam theory, Sādhanā, 45(1), 188. https://doi.org/10.1007/s12046-020-01425-y

[47] A. Benfrid, M.B. Bouiadjra, M. Chatbi, Z.R. Harrat (2024) Impact of glass nanoparticles on the elastic modulus of concrete, University of Zawia Journal of Engineering Sciences and Technology, 2(2), 182–188. https://doi.org/10.26629/uzjest.2024.16

[48] J. Ekpraseert, I. Fongkaew, P. Chainakun, R. Kamngam, W. Boonsuan (2020) Investigating mechanical properties and biocement application of $CaCO_3$ precipitated by a newly-isolated Lysinibacillus sp. WH using artificial neural networks, Scientific Reports, 10(1), 16137. https://doi.org/10.1038/s41598-020-73217-7

[49] S.B. Ghugal, I.I. Sayyad (2011) Free vibration of thick isotropic plates using trigonometric shear deformation theory, Journal of Solid Mechanics, 3(2), 172–182.

[50] I.I. Sayyad, S.B. Chikalthankar, V.M.B. Nandedkar (2013) Bending and free vibration analysis of isotropic plate using refined plate theory, Bonfring International Journal of Industrial Engineering and Management Science, 3(2).

[51] S. Kaewsit, K. Sompong, P. Pakawanit, W. Akkalatham, P. Yongsiri (2025) The study of light weight expanded clay aggregate from industrial waste, Chiang Mai Journal of Science, 52(5), e2025061. https://doi.org/10.12982/CMJS.2025.061

[52] S. Zhang, Z. Zhong, Z. Wang, Y. Dai, D. Niu, J. Liu et al. (2025) A piezoelectric stick-slip actuator

utilizing an asymmetric inertial driving foot: Design, analysis and experiments, Chiang Mai Journal of Science, 52(5), e2025062. https://doi.org/10.12982/CMJS.2025.062

[53] T. Chareerat, N. Nuanlert, J. Laorchan, N. Onputta, A. Pranudtaa, S. Rukzon et al. (2025) Effect of aggregate size and void ratio on plant growth in porous concrete-based hydroponic systems, Chiang Mai Journal of Science, 52(5), e2025073. https://doi.org/10.12982/CMJS.2025.073

[54] N. Dechboon, A. Wilai, P. Wilai, T. Tungyai (2025) Sustainability in celadon glazes using lampang kaolin waste and longan wood ash on the characteristics and heat-resistant properties for sankampang kiln wares, Chiang Mai Journal of Science, 52(4), e2025047. https://doi.org/10.12982/CMJS.2025.047

[55] S. Bello, T.O. Uthman, S. Surgun, A.M. Sokoto (2025) Characterization, compositional analysis and calorific value of Terminalia ivorensis sawdust, corncob and low-density polyethylene as potential blended feedstock for bio-oil production, Chiang Mai Journal of Science, 52(4), e2025056. https://doi.org/10.12982/CMJS.2025.056

[56] A.A. Al-Ani, N. Hilal, K. Muthusamy, M. Chatbi, Z.R. Harrat (2025) Static and dynamic analysis of bridge decks reinforced with nanoparticles, International Congress on Global Practice of Multidisciplinary Scientific Studies-X, Liberty Publications.

[57] A. Benfrid, M. Chatbi, Z.R. Harrat, M.B. Bouiadjra (2025) Selective integration of waste-derived glass nanopowders in structural wall concrete: Improving thermal efficiency and elasto-mechanical properties for sustainable construction, Periodica Polytechnica Civil Engineering, 69(3), 954–965. https://doi.org/10.3311/PPci.39913

[58] Z.R. Harrat, M. Chatbi, B. Krour, S. Amziane, M.B. Bouiadjra, M. Hadzima-Nyarko, D. Radu, E. Işık (2024) Bending analysis of nano-Fe_2O_3 reinforced concrete slabs exposed to temperature fields and supported by viscoelastic foundation, Advances in Concrete Construction, 17(2), 111–126. https://doi.org/10.12989/acc.2024.17.2.111

[59] M. Lakhder, A. Benfrid, M.B. Bouiadjra, M. Chatbi, Z.R. Harrat, A. Benbakhti (2025) The mechanical bending behavior of a new metal alloy nano-reinforced plate incorporating tungsten nano particles, NIPES – Journal of Science and Technology Research, 7(3), 423–440. https://doi.org/10.37933/nipes/7.3.2025.1682

[60] M. Chatbi, Z.R. Harrat, M.A. Benatta, B. Krour, M. Hadzima-Nyarko, E. Işık, S. Czarnecki, M.B. Bouiadjra (2023) Nano-clay platelet integration for enhanced bending performance of concrete beams resting on elastic foundation: An analytical investigation, Materials, 16(14), 5040. https://doi.org/10.3390/ma16145040

[61] B. Ahmed, A. Mohamed, S. Baghdad, B. Abdelmoutalib (2025) First-principles study of the structural, electronic, and elastic properties of hydride perovskites $XCaH_3$ (X = Na, K, Rb, Cs) under pressure, Veredas Do Direito, 22(2), e3223. https://doi.org/10.18623/rvd.v22.n2.3223

[62] H. Bouchehit, H. Torkia, A. Kadid, A. Benfrid (2025) Comparative seismic analysis of cylindrical and rectangular oil tanks: Effects of wall thickness under soil–structure–fluid interaction, Veredas Do Direito, 22(2), e3224. https://doi.org/10.18623/rvd.v22.n2.3224

[63] B. Ahmed, D. Hafida, R. Djihad, B. Abdelmoutalib (2025) Flexural performance of concrete beams incorporating granite waste, Veredas Do Direito, 22(2), e3155. https://doi.org/10.18623/rvd.v22.n2.3155

[64] A. Yerkrou, A. Benfrid, B. Krour, M.B. Bouiadjra (2025) A programming model for analyzing the mechanical and thermal buckling behavior of eco-concrete panels incorporating recycled waste materials, Veredas Do Direito, 22(2), e3117. https://doi.org/10.18623/rvd.v22.n2.3117

[65] B. Abdelmoutalib, K. Murawski, B. Samir (2025) Thermal instability of a polymer panel reinforced with glass particulates, ISPEC Journal of Science Institute, 4(2), 210–215. https://doi.org/10.5281/zenodo.18062068

[66] A. Benfrid (2026) Prediction of thermal and mechanical properties of eco-concretes using a biphasic homogenization approach, Zenodo. https://doi.org/10.5281/zenodo.19322922

[67] S. Belmahi, A. Benfrid, I. Klouche Djedid, R. Guergour, N. Djakhdane (2026) Influence of acidic and alkaline environments on the mechanical properties of cement mortars, Periodica Polytechnica Civil Engineering, 70(1), 315–326. https://doi.org/10.3311/PPci.42312

[68] A. Benfrid (2026) The elastomechanical properties of concrete expanded with aluminum nano-inclusions, Journal International Review of Research Studies, 1(2), 1–9. https://doi.org/10.66104/gkkj0g48

[69] H. Khetir, A. Benfrid, M.B. Bouiadjra, L. Melati (2026) Contribution to the mechanical performance of a simply supported lightweight concrete beam reinforced with bio-sourced nanocomposites, Revista Brasileira de Engenharia de Biossistemas, 19. https://doi.org/10.18011/bioeng.2025.v19.1293

[70] M. Chatbi, Z.R. Harrat, M.A. Benatta, B. Krour, M. Hadzima-Nyarko, E. Işık, S. Czarnecki, M.B. Bouiadjra (2023) Influence of nano-clay platelets on the bending response of concrete beams resting on elastic foundations, Materials, 16(14), 5040. https://doi.org/10.3390/ma16145040

[71] Z.R. Harrat, A. Achour, M. Chatbi, M. Hadzima-Nyarko, E. Işık (2026) Modelling the dynamic response of clay nanoparticle-modified concrete beams resting on two-parameter elastic foundations, Modelling, 7(2), 64. https://doi.org/10.3390/modelling7020064

[72] A. Zahafi, M. Hadid, R. Bencharif (2024) Lumped parameter model for vertical vibrations of surface circular foundations on nonhomogeneous soil, World Journal of Engineering, 21(4), 632–653. https://doi.org/10.1108/WJE-01-2023-0012

[73] R. Bencharif, A. Zahafi, N. Mezouar, M. Hadid (2023) Time-domain implementation of soil-structure interaction analysis techniques with

frequency-dependent impedance functions, Algérie Équipement, 69, 1–20.

[74] M. Chatbi, S. Lozančić, Z.R. Harrat, M. Hadzima-Nyarko (2026) Computational models for the vibration and modal analysis of silica nanoparticle-reinforced concrete slabs with elastic and viscoelastic foundation effects, Modelling, 7(1), 8. https://doi.org/10.3390/modelling7010008

[75] M. Chatbi, Z.R. Harrat, T. Ghazoul, M.B. Bouiadjra (2022) Free vibrational analysis of composite beams reinforced with randomly aligned and oriented carbon nanotubes, resting on an elastic foundation, Journal of Building Materials and Structures, 9(1), 22–32. https://doi.org/10.34118/jbms.v9i1.1895

[76] R. Bencharif, M. Hadid, N. Mezouar (2020) Hybrid BEM-TLM-PML method for the dynamic impedance functions calculation of a rigid strip-footing on a nearly saturated poroelastic soil profile, Engineering Analysis with Boundary Elements, 116, 31–47. https://doi.org/10.1016/j.enganabound.2020.03.001

[77] M.Y. Tebbouche, D. Ait Benamar, H.M. Hassan et al. (2022) Characterization of El Kherba landslide triggered by the August 07, 2020, Mw = 4.9 Mila earthquake (Algeria) based on post-event field observations and ambient noise analysis, Environmental Earth Sciences, 81, 46. https://doi.org/10.1007/s12665-022-10172-8

[78] A. Benfrid (2026) Évaluation théorique des propriétés effectives des bétons environnementaux : Une étude comparative des modèles d'homogénéisation, unpublished work.

[79] M. Sid Ahmed, A. Benfrid, A.S. Benosman, M. Hacini, M. Mouli, O. Taleb, A. Badache (2026) Analysis of thermally treated plastic-pozzolanic modified mortars and their mechanical properties, Zaštita Materijala, in press. https://doi.org/10.62638/ZasMat1595

[80] M. Sid Ahmed, M. Hacini, A.S. Benosman et al. (2026) Development of eco-friendly composite mortars for the circular economy and sustainable construction: Rheological, thermo-mechanical, durability characterization, and environmental impact assessment, Circular Economy and Sustainability, 6, 80. https://doi.org/10.1007/s43615-026-00747-z

[81] F. Turan, A. Benfrid (2025) Free vibration of higher-order shear deformable porous orthotropic beams, Conference on Engineering and Artificial Intelligence in Achieving Sustainable Development for Building the State, Libya, proceedings.

[82] A. Benfrid (2025) The free vibration of a building's raft foundation reinforced with short steel fibers, 15th International Mardin Artuklu Scientific Researches Conference, Mardin, Türkiye, proceedings.

[83] A. Benfrid, F. Turan (2025) Eco-friendly concrete: Thermal transfer study of panels with low concentrations of recycled cardboard, Conference on Engineering and Artificial Intelligence in Achieving Sustainable Development for Building the State, Libya, proceedings.

[84] K. Mladenov, A. Doicheva (2009) On some illustrative potentialities of simply supported beams, 11th National Congress on Theoretical and Applied Mechanics, Borovets, Bulgaria, proceedings. http://nctam.imbm.bas.bg/index.php/nctam/nctam2009/paper/viewFile/127/43

[85] K. Mladenov, A. Doicheva (2009) Flexural-torsional buckling of an off-centre supported beam, Annual of the University of Architecture, Civil Engineering and Geodesy, XLIV(V), 103–114.

[86] A. Doicheva (2011) Exact solution for a beam on off-center spring supports, Journal of Theoretical and Applied Mechanics, 41(2), 69–82.

[87] A. Doicheva (2016) T-shaped frame critical and post-critical analysis, Journal of Theoretical and Applied Mechanics, 46(1), 65–82.

[88] K. Mladenov, A. Doicheva (2016) Critical and post-critical analysis of water tower with conical tank, Annual of the University of Architecture, Civil Engineering and Geodesy, 49(2), 63–76.

[89] K. Mladenov, A. Doicheva (2008) Bending-torsional buckling of a beam on elastic rotational springs, Civil Engineering, 6, 2–7.

[90] A. Doicheva, K. Mladenov (2005) On some dynamic characteristics in the analysis of building structures, Scientific Conference with International Participation, Stara Zagora, Bulgaria, proceedings, 139–145.

[91] A. Doicheva (2024) Shear force of interior beam–column joints under symmetrical loading with two transverse forces on the beam, Buildings, 14(9), 3028. https://doi.org/10.3390/buildings14093028

[92] A. Doicheva (2024) Shear force in RC internal beam-column connections for a beam loaded with a transverse force occupying different possible positions, Eurasia Proceedings of Science, Technology, Engineering & Mathematics, 29, 128–144. https://doi.org/10.55549/epstem.1563437

[93] A. Doicheva (2024) Alteration of the shear force in an internal beam-column joint during the initiation and growth of a crack in a cantilever beam, Procedia Structural Integrity, 66, 433–448. https://doi.org/10.1016/j.prostr.2024.11.096

[94] A. Doicheva (2025) Repercussions on the shear force of an internal beam–column connection from two symmetrical uniformly distributed loads at different positions on the beam, Engineering Proceedings, 87, 85. https://doi.org/10.3390/engproc2025087085

[95] A. Doicheva (2025) Horizontal shear force in RC internal beam-column connection at initiation and crack growth from linearly distributed load on a cantilever beam, Procedia Structural Integrity, 72, 235–242. https://doi.org/10.1016/j.prostr.2025.08.098

[96] Anonymous (2025) A new approach for studying plaster beam bending based on DISS Algerian nano-short-bio-fibres, Modern Journal of Health and Applied Sciences, 2(1), 43–58. https://doi.org/10.70411/MJHAS.2.1.2025183

[97] A. Benfrid, M.B. Bouiadjra, Z.R. Harrat, F. Saoudi (2025) Thermal insulation using bio-based concrete made from apricot kernels, First National

Conference on Mechanical Applications, Centre universitaire Maghnia, Algeria, proceedings.
[98] A. Benfrid, M.B. Bouiadjra, F. Saoudi (2025) Enhancing thermal efficiency of bio-concrete with wheat straw nanofibers: A sustainable approach for energy-efficient buildings, 2nd Online National Conference on Materials Physics, El Tarf, Algeria, proceedings.
[99] .Benfrid, M. Chatbi, Z.R. Harrat, M.B. Bouiadjra (2025) Analytical evaluation of sustainable nano-reinforced concrete panels for improved thermo-mechanical performance, Conference on Sustainable Construction Materials, Algeria, proceedings.
[100] A. Benfrid, M.B. Bouiadjra, B. Krour, Z.R. Harrat (2025) Homogenization-based prediction of effective mechanical properties of bio-sourced concrete composites, Conference on Advanced Structures and Materials in Civil Engineering, Sidi Bel Abbes, Algeria, proceedings.

IZVOD

EFIKASNA MEHANIČKA SVOJSTVA EKO-BETONA ARMIRANIH NANOČESTICAMA KALCIJUM KARBONATA BIO-IZVORA: ANALIZA SLOBODNIH VIBRACIJA JEDNOSTAVNO OSLONJENIH PLOČA

Otpad bogat kalcijum karbonatom bio-izvora, kao što su ljuske jaja, riblje kosti, životinjske kosti i ljušture puževa, predstavlja obećavajuće sirovine za proizvodnju nanočestica kalcijum karbonata nakon odgovarajuće obrade, kao što su mlevenje, kalcinacija ili hemijsko taloženje. U ovoj studiji, ispitivana su efektivna mehanička svojstva i odziv slobodnih vibracija jednostavno oslonjenih eko-betonskih ploča armiranih nanočesticama kalcijum karbonata bio-izvora.
Efektivna elastična svojstva betonskog kompozita procenjena su korišćenjem Hašin-Štrikmanovog modela homogenizacije za dvofazni izotropni sistem sastavljen od betona kao matrice i nano-$CaCO_3$ čestica kao armature. Razmatrani su zapreminski udeo armature od 10% i 20%. Ponašanje armiranih ploča pri slobodnim vibracijama je zatim analizirano korišćenjem Teorije deformacije smicanja prvog reda (FSDT) i Teorije deformacije smicanja višeg reda (HSDT). Upravne jednačine su izvedene korišćenjem principa virtuelnog rada, a Navijeovo analitičko rešenje je usvojeno da bi se zadovoljili jednostavno oslonjeni granični uslovi.
Dobijeni rezultati pokazuju da dodavanje nano-$CaCO_3$ poboljšava efektivnu krutost betona. Jangov modul se povećava sa 20 GPa za običan beton na 22,81 GPa i 25,88 GPa za armaturu sa 10% i 20% nano-$CaCO_3$, respektivno. Osnovna bezdimenzionalna frekvencija kvadratne ploče povećava se sa 0,0921 za običan beton na 0,1277 i 0,1287 za 10% i 20% nano-$CaCO_3$, respektivno. Ovi rezultati ukazuju da 10% nano-$CaCO_3$ pruža značajno poboljšanje krutosti i vibracionih performansi, dok dodatni dobitak izvan ovog udela ostaje ograničen. Formulacija HSDT pokazuje bolje slaganje sa referentnim rezultatima nego FSDT i stoga je usvojena za parametarsku analizu.
Ključne reči: *Eko-beton, kalcijum karbonat bio-izvora, nano-$CaCO_3$, Hašin-Štrikmanov model, jednostavno oslonjena ploča, slobodne vibracije, HSDT.*

Naučni rad
Rad primljen: 22.04.2026.
Rad prihvaćen: 04.05.2026.

MOHAMMEDI Mohammed Nourelislam *: https://orcid.org/0009-0009-1324-4366*

BENFRID Abdelmoutalib *https://orcid.org/0009-0007-8171-1654*

BENATTA Mohamed Atef *https://orcid.org/ 0009-0007-5854-9054*

BACHIR BOUIADJRA Mohammed *https://orcid.org/0009-0008-4814-6187*

KROUR Baghdad *https://orcid.org/ 0000-0002-8265-9807*